

Black Hole Metamorphosis and Stabilization by Memory Burden

GIA DVALI^{*1,2}, LUKAS EISEMANN^{†1,2}, MARCO MICHEL^{‡1,2}, AND SEBASTIAN
ZELL^{§3,1,2}

¹*Arnold Sommerfeld Center, Ludwig-Maximilians-Universität,
Theresienstraße 37, 80333 München, Germany*

²*Max-Planck-Institut für Physik, Föhringer Ring 6, 80805 München, Germany*

³*Institute of Physics, Laboratory for Particle Physics and Cosmology, École Polytechnique
Fédérale de Lausanne, CH-1015 Lausanne, Switzerland*

November 29, 2021

Abstract

Systems of enhanced memory capacity are subjected to a universal effect of *memory burden*, which suppresses their decay. In this paper, we study a prototype model to show that memory burden can be overcome by rewriting stored quantum information from one set of degrees of freedom to another one. However, due to a suppressed rate of rewriting, the evolution becomes extremely slow compared to the initial stage. Applied to black holes, this predicts a metamorphosis, including a drastic deviation from Hawking evaporation, at the latest after losing half of the mass. This raises a tantalizing question about the fate of a black hole. As two likely options, it can either become extremely long lived or decay via a new classical instability into gravitational lumps. The first option would open up a new window for small primordial black holes as viable dark matter candidates.

*georgi.dvali@physik.uni-muenchen.de

†lukas.eisemann@physik.uni-muenchen.de

‡marco.michel@physik.uni-muenchen.de

§sebastian.zell@epfl.ch

Contents

1	Introduction	3
1.1	Big Picture	3
1.2	Main Finding	4
1.3	Outline	7
2	Enhanced Memory Storage: A Prototype Model	8
2.1	Assisted Gaplessness	8
2.2	Memory Burden	9
2.3	Avoiding Memory Burden by Rewriting	11
2.4	Bounds on Couplings	12
2.5	Application to Black Holes	13
3	Numerical Time Evolution	16
3.1	Possibility of Rewriting	17
3.2	Dependence on System Size	19
3.3	Application to Black Hole	20
3.4	Regime After Metamorphosis	22
4	Small Primordial Black Holes as Dark Matter	23
4.1	Effects on Bounds	23
4.2	Specific Example	24
5	Summary and Conclusions	26
5.1	Stabilization by Memory Burden	26
5.2	Black Hole Metamorphosis After Half Decay	27
A	Finding Parameter Scalings	28
A.1	N_c -Scaling	29

A.2	ϵ_m -Scaling	29
A.3	C_0 -Scaling	30
A.4	ΔN_c -Scaling	30
A.5	K -Scaling	31

1 Introduction

1.1 Big Picture

This paper is about understanding a very general phenomenon [1, 2], called *memory burden*, exhibited by systems that achieve a *high capacity of memory storage* and its potential applications to black holes. The essence of the story is that a high load of quantum information carried by such a system stabilizes it. This means that, in order to decay, the system must off-load the memory pattern from one set of modes into another one. Our studies show that this becomes harder and harder with larger size. As a result, the quantum information stored in the memory back-reacts and stabilizes the system at the latest after its half-decay. The universality of the phenomenon suggests its natural application to black holes.

The present paper is a part of a general program, initiated some time ago, which consists of two main directions. One is the development of a microscopic theory describing a black hole as a bound state of soft gravitons, a so-called quantum N -portrait [3]. The occupation number N_c of gravitons is critical in the sense that it is the inverse of their (dimensionless) gravitational interaction. The softness of gravitons here refers to wavelengths comparable to the gravitational radius of a black hole. This criticality has been identified [4] as the key reason for understanding the maximal information storage capacity of a black hole quantified by its Bekenstein-Hawking entropy. Due to extremely weak interactions among the constituent gravitons, this framework allows to perform computations within the validity domain of effective field theory exploiting the power of $1/N_c$ -expansions.

The second direction [1, 2, 4–11] is to instead use the *enhanced capacity of memory storage* as a guiding principle. That is, we study generic systems which possess states with a high capacity of memory storage and try to identify universal phenomena that take place near such states. The idea then is to come back and apply this knowledge to black holes and look for analogous phenomena there. The advantage of this approach is that a unique knowledge about black holes can be gained by studying systems that are much easier solvable both analytically and numerically. The present paper is about the detailed study of one such universal phenomenon identified in [1, 2], namely the above mentioned memory burden.

Before continuing we wish to make a clarifying remark, in order not to confuse the reader with our terminology. We shall often use the term *enhanced capacity of the memory storage* as opposed to, for example, *maximal entropy*. This is because the former term

covers a wider class of systems: A state can have a sharply enhanced memory storage capacity even if the corresponding microstate entropy is not necessarily maximal. The above studies show that systems that possess such states still exhibit some black hole like properties. Of course, the converse is in general true: A state of maximal microstate entropy does possess a maximal memory storage capacity. In particular, all such states must share the memory burden effect.

1.2 Main Finding

Let us start with setting the framework. Physical systems are characterized by a set of degrees of freedom (modes) and interactions between them. It is convenient and customary to describe the degrees of freedom as quantum oscillators. The basic quantum states of the system then can be labeled by a sequence of their occupation numbers $|n_1, \dots, n_K\rangle$. Such a sequence stores quantum information which we can refer to as the *memory pattern*. The efficiency of memory storage is then measured by the number of patterns that can be stored within a certain microscopic energy gap [9, 10]. When this number is high, we shall say that the system has an enhanced capacity of memory storage. The above notion is closely related to microstate entropy but is much more general. If the states describing different patterns share the same macroscopic characteristics (e.g., the total mass or angular momentum), the microstate entropy can be defined in the usual way $S = \ln(n_{\text{st}})$, where n_{st} is the number of distinct basic microstates $|n_1, \dots, n_K\rangle$.

Naturally, we are interested in systems that dynamically attain a high capacity of memory storage. This can be achieved if the system reaches a critical state in which a large number of gapless modes emerge. Then an information can be encoded in the occupation numbers of the gapless modes without energy cost. This generic mechanism has already been investigated in a series of papers [1, 2, 4, 5, 7–10]. Originally, it was introduced for understanding the origin of Bekenstein-Hawking entropy in a microscopic theory of black hole’s quantum N -portrait [3]. However, it was soon realized in the above papers that this mechanism is universally operative in systems with high capacity of memory storage. Interestingly, it has been repeatedly observed that the information storage in such systems exhibits some black hole-like properties.

This universality suggests that by understanding general phenomena and applying this understanding to black holes, we can gain new knowledge that until now has been completely blurred by technical difficulties in quantum gravity computations. Such *terra incognita* is the black hole evolution beyond its half evaporation. The reason is that the standard semi-classical computations are unable to account for quantum back reaction. Therefore, they are no longer applicable once back reaction becomes important, i.e., the latest by half evaporation. Instead, for resolving such questions a microscopic theory is needed such as quantum N -portrait [3].

As mentioned above, in this microscopic theory the black hole is described as a saturated critical state of soft gravitons of wavelengths given by the gravitational radius of a black hole, r_g . Since the occupation number is critical, i.e., equal to the inverse of their gravitational coupling, the kinetic energy of individual gravitons just saturates

the collective attraction from the rest. As a result, the gravitons form a long-lived bound-state, a black hole. However, the bound-state is not eternal. Instead, due to their quantum re-scattering, the soft bound-state slowly loses its constituents and depletes. On average, it emits a quantum of wavelength r_g per time r_g . At the same time, the emissions of quanta that are either much harder or softer are suppressed. In total, this process reproduces Hawking's evaporation up to $1/N_c$ corrections. It is these $1/N_c$ -corrections that are responsible for new effects that were invisible in the standard semi-classical treatment. Note that the latter corresponds to the $N_c = \infty$ limit of the microscopic theory.

The computations performed in the microscopic theory [12–16] unambiguously indicate that the classical description breaks down after the black hole has lost on the order of half of its mass, which corresponds to on the order of $N_c/2$ emissions. At this point, the back reaction (i.e., $1/N_c$ -effects integrated over time) become so important that the true quantum evolution completely departs from the naive semi-classical one. In this light, the two immediate tasks are: 1) Better quantify the quantum back reaction effects that lead to this breakdown; and 2) Predict what happens beyond this point.

In order to address these questions, we shall try to understand very general aspects of time-evolution of systems of enhanced memory capacity. We shall use the simplest possible prototype model with this property. Then we try to extend the obtained knowledge to black holes and cosmology and speculate about the possible consequences. The above strategy is the continuation of the one adopted in the previous papers [1,2,4–11]. The persistent pattern emerging from this work is that systems of enhanced capacity of memory storage exhibit striking similarities with certain black hole properties. For example, they share a slow initial decay via the emission of the soft quanta without releasing the stored information for a very long time. In short, it appears to be a promising strategy to try to make progress in understanding black holes by abstracting from the geometry and instead viewing their information storage capacity as the key characteristic.

In order to avoid any misunderstanding, we wish to clearly separate solid results from speculations. In the present paper, we shall focus on a very precise source of quantum back reaction. Following [1,2], we shall refer to it as the phenomenon of *memory burden*. The essence of it, as described above, is that the high load of quantum information stored in a memory pattern tends to stabilize the system in the state of enhanced memory capacity. We shall show that the strength of the effect maximizes at the latest by the time the system emits half of its energy. At the same time, the information stored in the memory becomes accessible. Because of very transparent physical mechanism behind these findings, it is almost obvious that it must be shared by generic systems of enhanced memory capacity, including black holes and de Sitter Hubble patch. This means that the tendency of a growing back reaction from the memory burden must be applicable to such objects. It is therefore expected that the back reaction from a stored quantum information must drastically modify the semi-classical picture by half-decay.

Note that this statement is in no conflict with any known black hole property derived in semi-classical theory. The reason, as already predicted both by calculations in gravitational microscopic theory [12–16] as well as by analysis of the prototype mod-

els [1, 2, 4–11] including the present paper, is that after losing half of the mass the semi-classical description is no longer applicable. Namely:

An old black hole that lost half of its mass is by no means equivalent to a young classical black hole of the equal mass.

In other words, the quantum effects such as the memory burden provide a universal *quantum clock* that breaks the self-similarity of black hole evaporation and suppresses its quantum decay. This is the key result of the present paper.

Some applications of this phenomenon to inflationary cosmology were already discussed in [2]. It was pointed out there that the memory burden of the primordial information carried by degrees of freedom responsible for Gibbons-Hawking entropy [17] can provide a new type of the *cosmic quantum hair*. This hair imprints a primordial quantum information from the early stages of inflation past last the 60 e-foldings.

Now, the speculative part of our paper concerns the extrapolation of the stabilization tendency for a black hole beyond its half-decay. At the present level of understanding, such an extrapolation is a pure speculation since strictly speaking there is no guarantee that universality of the phenomenon holds on such long timescales. In particular, it remains a viable option that after losing on the order of half of its mass via quantum emission, a new classical instability can set in. The black hole then can fall apart via a highly non-linear classical process.

Our precautions can be explained in the following way. The state of maximal memory capacity represents a type of criticality. The behavior of the system is then fully controlled by the gapless spectrum that emerges in this state. This explains the universal behavior of very different systems that exist in such a state. However, after half-decay the departure from the critical state is significant and it is conceivable that different systems behave differently after this point. So, despite the fact that our prototype model gets stabilized, a real black hole could follow a different path.

In summary, the following two natural possibilities emerge:

- The black hole continues its quantum decay but with an extremely-suppressed emission rate.
- A classical instability sets in and the black hole decays into highly non-linear graviton lumps, a sort of a gravitational burst.

While both outcomes would obviously have spectacular consequences, in the present paper we shall speculate more on the first option. That is, we can take the stabilization exhibited by the prototype model as a circumstantial evidence indicating that large black holes (i.e., $N_c \gg 1$, meaning much heavier than the Planck mass) behave in a similar manner, at least qualitatively. Therefore, the decay rate of *macroscopic* black holes could fall drastically after they lose half of their mass. Not surprisingly, the consequences of such stabilization would be dramatic. One obvious application that shall be discussed later is for primordial black holes as dark matter candidates.

1.3 Outline

We shall now briefly outline our analysis in more technical terms. The first ingredient is to explain the essence of the universal mechanism which allows the system to reach the state of enhanced memory storage. This mechanism is at work in large class of systems [1, 2, 4–10]. Following [10], we shall refer to it as *assisted gaplessness*. The essence of this mechanism is most transparently explained by a simple model discussed in [1, 2, 7–9], which we shall adopt as the prototype system in our analysis. The idea is that a high occupation of a particular low-frequency mode to a certain critical level, renders a large set of other would-be-high-frequency modes gapless. Namely, the highly-occupied *master mode* interacts attractively with a set of other modes. We shall call the latter degrees of freedom the *memory modes*. Near the vacuum, the memory modes would have high energy gaps and would be useless (i.e., energetically costly) for storing information. However, coupling to the master mode lowers their energy gaps when the latter is highly occupied. That is, the attractive coupling with the master mode translates as a negative contribution to the energy of the memory modes. As soon as the occupation number of the master mode reaches a critical level N_c , it can balance their positive kinetic energies. In this way, the memory modes become effectively gapless. Consequently, the states that correspond to different occupation numbers of these modes, $|n_1, \dots, n_K\rangle$, are degenerate in energy and contribute into the microstate entropy S .

So far, we have discussed how the master mode influences the memory modes by making them effectively gapless. However, the memory modes also backreact on the master mode via the effect of *memory burden* [1, 2]. Since the memory modes are gapless exclusively for a critical occupation N_c of the master mode, any evolution of the latter away from such a state would cost a lot of energy. Therefore, the system backreacts on the master mode and resists to the change of its occupation number N_c .

The next step in this line of research is to study to what extent the memory burden can be avoided. Namely, it has been proposed in [1] that it can be alleviated if the system has a possibility of rewriting the stored information from one set of modes to another. This could happen if another set of memory modes exists, which becomes gapless at a different occupation number N'_c of the master mode. Then, it is in principle conceivable that the occupation N_c changes in time, provided this change is accompanied by rewriting of the stored information from the first set of the memory modes to the second one. However, it has not yet been studied if such a rewriting is dynamically possible.

In order to attack the issue, we can split this question in two parts.

1. Does rewriting take place at all and under what conditions?
2. If the answer to the first question is positive, what is the timescale of this process?

Answering these questions is the goal of the present work.

In section 2, we will summarize some of the findings of [1, 2, 4–10] and develop a con-

crete prototype model that possesses states of enhanced memory capacity. Moreover, we discuss how it can be mapped on a black hole. In section 3, we investigate the prototype model numerically and in particular study rewriting between two different sets of memory modes. In short, we confirm that such a possibility can be realized dynamically. However, we discover that the speed of transition decreases as the size of the system increases. Applied to black holes, this indicates that evaporation has to slow down at the latest after they have lost half of their mass. In section 4, we discuss resulting consequences for primordial black holes as dark matter candidates. We give an outlook in section 5 and appendix A contains details as to how the speed of rewriting depends on the various parameters of the system.

2 Enhanced Memory Storage: A Prototype Model

2.1 Assisted Gaplessness

Following [8–10], we shall construct a simple prototype model that dynamically achieves a state with many gapless modes and correspondingly a high microstate entropy S . We consider K bosonic modes, which we describe by the usual creation and annihilation operators $\hat{a}_k^\dagger, \hat{a}_k$, where $k = 1, \dots, K$. They satisfy standard commutation relations (here and throughout $\hbar = 1$):

$$[\hat{a}_j, \hat{a}_k^\dagger] = \delta_{jk}, \quad [\hat{a}_j, \hat{a}_k] = [\hat{a}_j^\dagger, \hat{a}_k^\dagger] = 0, \quad (1)$$

and the corresponding number operators are given as $\hat{n}_k = \hat{a}_k^\dagger \hat{a}_k$. We denote its eigenstates by $|n_k\rangle$, where n_k is the eigenvalue. Moreover, we label the energy gap of \hat{n}_k by ϵ_k .

Using the modes \hat{n}_k , one can form the states

$$|n_1, \dots, n_K\rangle \equiv |n_1\rangle \otimes |n_2\rangle \otimes \dots \otimes |n_K\rangle, \quad (2)$$

where n_1, \dots, n_K can take arbitrary values. Clearly, the number of such states scales exponentially with K , so for $K \gtrsim S$, their number reaches the required number of microstates. However, it is important to consider the energy of the states (2). Namely, two different states $|n_1, \dots, n_S\rangle$ and $|n'_1, \dots, n'_S\rangle$ differ by the energy $\Delta E = \sum_{k=1}^K \epsilon_k (n_k - n'_k)$. So unless the ϵ_k are extremely small, the states corresponding to different occupation numbers of the modes \hat{n}_k are not degenerate in energy. Therefore, they cannot contribute to a microstate entropy.

We can change this situation by introducing another mode \hat{n}_0 , with creation and annihilation operators $\hat{a}_0^\dagger, \hat{a}_0$ and commutation relations analogous to Eq. (1). The key point is that we add an attractive interaction between the mode \hat{n}_0 and all other modes:

$$\hat{H} = \epsilon_0 \hat{n}_0 + \left(1 - \frac{\hat{n}_0}{N_c}\right) \sum_{k=1}^K \epsilon_k \hat{n}_k, \quad (3)$$

where we parameterize the strength of the interaction by $1/N_c$ with $N_c \gg 1$. As long as \hat{n}_0 is not occupied, the gaps of the \hat{n}_k -modes are still given by ϵ_k . As soon as we

populate \hat{n}_0 , however, the effective gaps \mathcal{E}_k of the \hat{n}_k -modes are lowered:

$$\mathcal{E}_k = \left(1 - \frac{n_0}{N_c}\right) \epsilon_k. \quad (4)$$

Once a critical occupation $n_0 = N_c$ is reached, all modes \hat{n}_k become effectively gapless, $\mathcal{E}_k = 0$.

Therefore, all states of the form

$$|\underbrace{N_c}_{n_0}, n_1, \dots, n_K\rangle \quad (5)$$

are degenerate in energy for arbitrary values of n_1, \dots, n_K . In this situation, \hat{n}_0 is the master mode, which assists the memory modes $\hat{n}_1, \dots, \hat{n}_K$ in becoming gapless. We note, however, that one has to invest the energy $\epsilon_0 N_c$ to achieve gaplessness. If each of the memory modes can have a maximal occupation of d , this leads to a number of $(d+1)^K$ distinct states that possess the same energy, i.e., an entropy

$$S = K \ln(d+1). \quad (6)$$

In this way, a large number $K \approx S$ of nearly-gapless modes leads to the entropy S .

2.2 Memory Burden

Following [1,2], we next investigate the effect of memory burden, i.e., how the memory modes backreact on the master mode. To this end, we add another mode with which \hat{n}_0 can exchange occupation number. We denote its creation and annihilation operators by $\hat{b}_0^\dagger, \hat{b}_0$ with commutation relations analogous to Eq. (1) and $\hat{m}_0 = \hat{b}_0^\dagger \hat{b}_0$ is the corresponding number operator. Then the Hamiltonian becomes

$$\hat{H} = \epsilon_0 \hat{n}_0 + \epsilon_0 \hat{m}_0 + \left(1 - \frac{\hat{n}_0}{N_c}\right) \sum_{k=1}^K \epsilon_k \hat{n}_k + C_0 \left(\hat{a}_0^\dagger \hat{b}_0 + \hat{b}_0^\dagger \hat{a}_0\right), \quad (7)$$

where C_0 parametrizes the strength of interaction between \hat{n}_0 and \hat{m}_0 . We choose the gap of \hat{n}_0 and \hat{m}_0 to be equal in order to facilitate the oscillations between them.

Now we consider the initial state

$$|\text{in}_1\rangle = |\underbrace{N_c}_{n_0}, \underbrace{0}_{m_0}, n_1, \dots, n_K\rangle. \quad (8)$$

Since the occupation number of each of the memory modes is conserved in time, it is possible to solve the system analytically. For the expectation value of \hat{n}_0 , one obtains [1]:

$$n_0(t) = N_c \left(1 - \frac{4C_0^2}{4C_0^2 + \mu^2} \sin^2(\sqrt{C_0^2 + \mu^2/4} t)\right), \quad (9)$$

where we defined

$$\mu = - \sum_{k=1}^K \epsilon_k n_k / N_c. \quad (10)$$

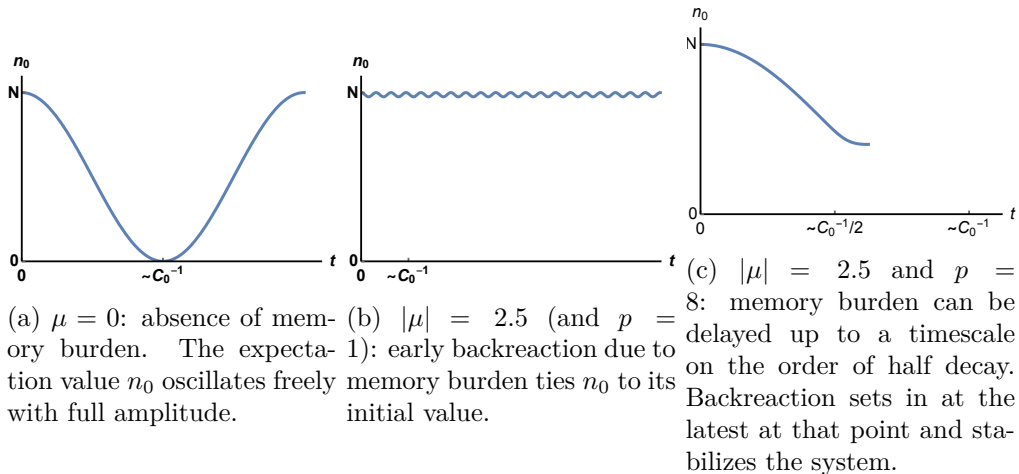


Figure 1: Plots of the time evolution of n_0 for $N_c = 25$ and $C_0 = \epsilon_0/\sqrt{N_c} = 1/5$. Figs. 1a and 1b follow from (9). Fig. 1c is an approximate solution of the system (12).

This quantity characterizes the strength of memory burden, as we shall demonstrate. It is related to the effective energy gaps (4) as

$$\mu = \sum_{k=1}^K n_k \frac{\partial \mathcal{E}_k}{\partial n_0}. \quad (11)$$

Eq. (9) shows that the memory modes drastically influence the time evolution of \hat{n}_0 . First, we consider the special situation in which all memory modes are unoccupied. This implies $\mu = 0$ so that $n_0(t)$ performs oscillation with maximal amplitude on a time scale of C_0^{-1} . This behavior, which is depicted in Fig. 1a, is identical to the case in which the memory modes do not exist. For $n_k \neq 0$, this situation changes as soon as either the occupation of the memory modes is high enough or their free gaps ϵ_k are sufficiently big. In both cases, one gets $C_0^2/\mu^2 \ll 1$ so that the amplitude of oscillations is suppressed by this ratio. This is shown in Fig. 1b for exemplary values of the parameters. Thus, the stored information ties \hat{n}_0 to its initial state. This is the essence of memory burden.

Consequently, the crucial question arises to what extent memory burden can be avoided. Following [2], a first way consists in modifying the Hamiltonian (7) as follows:

$$\hat{H} = \epsilon_0 \hat{n}_0 + \epsilon_0 \hat{m}_0 + \left(1 - \frac{\hat{n}_0}{N_c}\right)^p \sum_{k=1}^K \epsilon_k \hat{n}_k + C_0 \left(\hat{a}_0^\dagger \hat{b}_0 + \hat{b}_0^\dagger \hat{a}_0\right). \quad (12)$$

In this case, the effective energy gaps read

$$\tilde{\mathcal{E}}_k = \left(1 - \frac{n_0}{N_c}\right)^p \epsilon_k. \quad (13)$$

Consequently, the memory burden becomes

$$\tilde{\mu} = p \left(\frac{N_c - n_0}{N_c}\right)^{p-1} \mu, \quad (14)$$

where we expressed it in terms of Eq. (10). We see that it gets suppressed by powers of $(N_c - n_0)/N_c$. The larger p is, the more the backreaction gets delayed. However, it sets in at the latest when $\tilde{\mu}$ assumes the critical value C_0 :

$$N_c - n_0 = N_c \left(\frac{C_0}{p|\mu|} \right)^{1/(p-1)}. \quad (15)$$

For $\mu > C_0$, it is clear that memory burden can no longer be avoided as soon as $N_c - n_0$ is of the order of N_c . Thus, backreaction becomes important and the system stabilizes at the latest after a timescale on the order of half decay, as is exemplified in Fig. 1c.

2.3 Avoiding Memory Burden by Rewriting

In [1], another way of alleviating memory burden was proposed. The idea is to introduce a second sector of memory modes, which are not occupied in the beginning, but which can exchange occupation number with the first sector. If the coupling of the second sector to the master mode is such that it becomes gapless for a smaller value $n_0 = N_c - \Delta N_c$, then a final state in which n_0 has diminished by ΔN_c and all excitations have been transferred from the first to the second memory sector becomes energetically available.

We denote the creation and annihilation operators of the second memory sector by $\hat{a}'_{k'}$, $\hat{a}'_{k'}$, the number operator by $\hat{n}'_{k'} = \hat{a}'_{k'} \hat{a}'_{k'}$ and assume the usual commutation relations (1), where $k' = 1, \dots, K'$. Then the Hamiltonian becomes:

$$\begin{aligned} \hat{H} = & \epsilon_0 \hat{n}_0 + \epsilon_0 \hat{m}_0 + \left(1 - \frac{\hat{n}_0}{N_c} \right) \sum_{k=1}^K \epsilon_k \hat{n}_k + C_0 \left(\hat{a}_0^\dagger \hat{b}_0 + \hat{b}_0^\dagger \hat{a}_0 \right) \\ & + \left(1 - \frac{\hat{n}_0}{N_c - \Delta N} \right) \sum_{k'=1}^{K'} \epsilon_{k'} \hat{n}'_{k'} + \sum_{k=1}^K \sum_{k'=1}^{K'} C_{k,k'} \left(\hat{a}_k^\dagger \hat{a}'_{k'} + \text{h.c.} \right) \\ & + \sum_{k=1}^K \sum_{\substack{l=1 \\ l \neq k}}^K \tilde{C}_{k,l} \left(\hat{a}_k^\dagger \hat{a}_l + \text{h.c.} \right) + \sum_{k'=1}^{K'} \sum_{\substack{l'=1 \\ l' \neq k'}}^{K'} \tilde{C}_{k',l'} \left(\hat{a}'_{k'} \hat{a}'_{l'} + \text{h.c.} \right). \end{aligned} \quad (16)$$

Here the parameters $C_{k,k'}$ determine the strength of coupling between the two memory sectors. For completeness, we have moreover introduced interactions within each memory sector, the strength of which is set by $\tilde{C}_{k,l}$.

We consider an initial state in which the first memory sector is gapless and only the first sector is occupied:

$$|\text{in}\rangle = \left| \underbrace{N_c}_{n_0}, \underbrace{0}_{m_0}, n_1, \dots, n_K, \underbrace{0}_{n'_1}, \dots, \underbrace{0}_{n'_{K'}} \right\rangle. \quad (17)$$

As explained, a final state is energetically available in which the second memory sector is gapless and only the second sector is occupied:

$$|\text{out}\rangle = \left| \underbrace{N_c - \Delta N}_{n_0}, \underbrace{\Delta N}_{m_0}, \underbrace{0}_{n_1}, \dots, \underbrace{0}_{n_K}, n'_1, \dots, n'_{K'} \right\rangle. \quad (18)$$

The total occupation in the two memory sectors,

$$N_m \equiv \sum_{k=1}^K n_k + \sum_{k'=1}^{K'} n_{k'}, \quad (19)$$

is conserved.

However, so far the amplitude for a transition from $|\text{in}\rangle$ to $|\text{out}\rangle$ has not been investigated, i.e., it remains to be studied if the system can dynamically evolve from $|\text{in}\rangle$ to $|\text{out}\rangle$.

2.4 Bounds on Couplings

Before we investigate the time evolution, we study how large the couplings of the memory modes can be. Namely, they must fulfill the condition that the effective gap \mathcal{E}_{eff} of the memory modes stays close to zero in the presence of couplings. In order to obtain the mildest possible bound, we can consider a situation in which the gaps can equally be offset to positive or negative values. Consequently, occupying N_m modes typically only gives an energy disturbance of $\sqrt{N_m}\mathcal{E}_{\text{eff}}$. Imposing that it is smaller than the elementary gap, we obtain the constraint

$$\mathcal{E}_{\text{eff}} \lesssim \frac{\epsilon_0}{\sqrt{N_m}}. \quad (20)$$

First, we will turn to the coupling $\tilde{C}_{k,l}$ within one memory sector, where we assume that all $\tilde{C}_{k,l}$ are of the same order. If we only consider two modes for a moment, they are described by the effective coupling matrix

$$\begin{pmatrix} 0 & \tilde{C}_{k,l} \\ \tilde{C}_{k,l} & 0 \end{pmatrix}. \quad (21)$$

Thus, disturbing the gap by at most $\epsilon_0/\sqrt{N_m}$ implies $\tilde{C}_{k,l} \lesssim \epsilon_0/\sqrt{N_m}$. However, we need to take into account that it couples to many modes. When we view the couplings within one memory sector as samples from identical independent distributions with zero mean and unit variance, then the corresponding matrix, i.e., the generalization of Eq. (21) to many modes, belongs to a Wigner Hermitian matrix ensemble. In this situation, Wigner's semicircle law states that the spectral distribution converges, and in particular becomes independent of the dimension K , if the entries of the matrix are rescaled by $1/\sqrt{K}$ (see e.g., [18]). Thus, we need to suppress the coupling constants with this factor to maintain approximate gaplessness for the majority of modes:

$$\tilde{C}_{k,l} \lesssim \frac{\epsilon_0}{\sqrt{N_m}\sqrt{K}}. \quad (22)$$

We can also arrive at the same conclusion by studying the expectation value of the off-diagonal elements in the Hamiltonian, as was done in [19]. This energy scales as $N_m\tilde{C}_{k,l}$, where we took into account that N_m^2 non-zero entries only give a contribution on the

order of N_m as long as there are both positive and negative summands. Requiring this energy to be smaller than ϵ_0 yields

$$\tilde{C}_{k,l} \lesssim \frac{\epsilon_0}{N_m}. \quad (23)$$

For a typical occupation $N_m \sim K$, this bound is identical to Eq. (22)

Next, we study the coupling $C_{k,k'}$ of modes from different memory sectors, where we assume again that all $C_{k,k'}$ are of the same order. In this case, we get the effective coupling matrix

$$\begin{pmatrix} 0 & C_{k,k'} \\ C_{k,k'} & \epsilon_k \Delta N / N \end{pmatrix}. \quad (24)$$

We estimate $\mathcal{E}_{\text{eff}} \sim K C_{k,k'}^2 N / (\epsilon_k \Delta N)$. This gives the constraint

$$C_{k,k'} \lesssim \frac{\sqrt{\epsilon_0 \epsilon_k \Delta N}}{\sqrt{KN} (N_m)^{1/4}}, \quad (25)$$

which is milder than the bound (22) since $\epsilon_k \geq \epsilon_0$.

2.5 Application to Black Holes

We now wish to apply our results to black holes. Naturally, we shall work under the assumption that the above quantum system of enhanced memory capacity captures some very general properties of black hole information storage. Ideally, we would like not to be confined to any particular microscopic theory but rather to make use of certain universal properties that any such theory must incorporate. For example, existence of modes that become gapless around a macrostate corresponding to a black hole is expected to be such universal property. Indeed, without gapless excitations, it would be impossible to account for the black hole microstate entropy. Also, an important fact is that the Bekenstein-Hawking entropy [20] depends on the black hole mass M ,

$$S = 4\pi G_N M^2, \quad (26)$$

where G_N is Newton's constant. Correspondingly, the number of the gapless modes that a black hole supports depends on its mass. This makes it obvious that any evolution that decreases the black hole mass must affect the energy gaps of the memory modes. That is, when a black hole evaporates, some of the modes that were previously gapless now must acquire the energy gaps. But then, this process must result into a memory burden effect that resists against the decrease of M . This is the main lesson that we learn about black holes from our analysis. For more quantitative understanding, we shall try to choose the parameters of the above toy model to be maximally close to the corresponding black hole characteristics.

For a crude guideline, it will be useful to keep in mind a particular microscopic theory of black hole quantum N -portrait [3]. Although we wish to keep our analysis maximally general, having a microscopic theory helps in establishing a precise dictionary between parameters of a black hole and the presented simple Hamiltonian. It also shows how well the seemingly toy model captures the essence of the phenomenon.

According to quantum N -portrait, a black hole of Schwarzschild radius $r_g = 2G_N M$, represent a saturated bound-state of soft gravitons. The characteristic wavelength of gravitons contributing into the gravitational self-energy is given by r_g . These constituent gravitons play the role of the master mode. Namely, their occupation number is critical and this renders a set of other modes gapless. The latter modes play the role of the memory modes. Without the presence of a critical occupation number of the master mode, the memory modes would represent free gravitons of very high frequencies and respectively would possess very high energy gaps. That is, it would be very costly in energy to excite those modes if the occupation number of the master mode were not critical. Now, the idea is that these gapless modes account for the Bekenstein-Hawking entropy (26). In the above toy model, the role of the master mode is played by \hat{a}_0 with occupation number n_0 .

In this picture, the Hawking radiation [21] is a result of quantum depletion. Consequently, some of the particles of the master mode get converted into free quanta and the occupation number of the master mode decreases. These free Hawking quanta are impersonated by the quanta of mode \hat{b}_0 and they have the occupation number m_0 . Initially, $m_0 = 0$. However, during the conversion the occupation number m_0 increases while n_0 decreases and moves away from the critical value. This is expected to create a memory burden effect. Of course, unlike a black hole, the model (16) performs oscillations, i.e., \hat{m}_0 again loses quanta after a certain timescale. Thus, we can map our model on a black hole only up to this point, but this fully suffices for our conclusions.¹ Another reason why the timescale of validity of our model is limited is that black holes can exist for all values of the mass M . Therefore, a tower of sets of momentum modes has to exist so that one of them becomes gapless for each value of M . In contrast, we only consider two sets of momentum modes in our model. For this reason, our model can no longer be mapped on a black hole as soon as a third set of momentum modes would start to be populated.

We can now choose the parameters in such a way that Hamiltonian (16) reproduces the generic information-theoretic properties of a black hole. First, we set the elementary gap as $\epsilon_0 = r_g^{-1}$ to make sure that Hawking quanta have the correct typical energy r_g^{-1} . Next, we need $K = S$ to obtain the desired entropy. Consequently, a typical pattern has $N_m = S/2$, since for large black holes $S \gg 1$ and the number of patterns with different N_m is insignificant. We can also estimate the gap of the memory modes. Since the system is spherically symmetric, we can label states by the quantum numbers (l, m) of angular harmonics. Assuming no significant part of the energy of the modes is in radial motion, we need to occupy states at least until $l \sim \sqrt{K}$ in order to obtain a number of K modes, since the degeneracy of each level scales as l . In this case, the highest mode has an energy of $\epsilon_k = \sqrt{K}\epsilon_0$. We use this scale to estimate the free gap of the memory modes because the relative split in energy among the levels is inessential for our discussion. We remark that this means that those modes are Planckian, $\epsilon_k \sim 1/\sqrt{G_N}$. Finally, we have freedom in choosing the critical occupation number N_c . For concreteness, we set

¹The bilinear coupling between modes is motivated as the simplest possible coupling that is able to effectively describe energy transfer between degrees of freedom. In order to model a decay more precisely, one could instead consider a coupling to many species, $\frac{C_0}{\sqrt{F}} \sum_{f=1}^F \hat{a}_0 \hat{b}_f^\dagger + h.c.$ (all with the same gap $\epsilon_f = \epsilon_0$), which could e.g., represent momentum modes of a field-theoretic system. In the limit of large F , one can achieve strict decay with the same rate as in (16).

$N_c = S$, as is motivated by the quantum N-portrait. In this way, the total energy of the system reproduces the mass of the black hole: $M = N_c \epsilon_0$. In summary, we can express all quantities in terms of the entropy and the Schwarzschild radius:

$$\epsilon_0 = r_g^{-1}, \quad N_c = S, \quad K = S, \quad N_m = S/2, \quad \epsilon_k = \sqrt{S} r_g^{-1}. \quad (27)$$

Since gravitational coupling is universal, all $C_{k,k'}$ and all $\tilde{C}_{k,l}$ need to be of the same order. So Eq. (22) gives the strongest constraint, which reads

$$C_{k,k'} \sim \tilde{C}_{k,l} \lesssim \frac{\epsilon_0}{S}. \quad (28)$$

As stated before, this bound is the softest possible one. In real black holes constraints may be stronger.

When applying our analysis to real black holes, some additional facts must be taken into account. Namely, together with the \hat{b}_0 -mode, which impersonates the outgoing free quanta of Hawking radiation, there are also the free modes of higher momenta. In particular, there will of course exist the free modes of the same momenta k as the memory modes \hat{a}_k . These modes are denoted by \hat{b}_k . Now, unlike the memory \hat{a}_k -modes, the \hat{b}_k -modes are *not* subjected to the assisted gaplessness. Correspondingly, they satisfy the dispersion relations of free quanta. That is, the frequencies ϵ_k of \hat{b}_k -modes are of order of their momenta and, therefore, are much higher than the frequencies of the corresponding \hat{a}_k -modes. The essence of the situation is described by the following Hamiltonian

$$\hat{H}_{\text{higher}} = \sum_{k=1}^K \epsilon_k \hat{b}_k^\dagger \hat{b}_k + \sum_{k=1}^K C_k \left(\hat{a}_k^\dagger \hat{b}_k + \hat{b}_k^\dagger \hat{a}_k \right) + \sum_{k'=1}^{K'} C_{k'} \left(\hat{a}_{k'}^\dagger \hat{b}_{k'} + \hat{b}_{k'}^\dagger \hat{a}_{k'} \right). \quad (29)$$

As before, we have $\epsilon_k = \sqrt{S} \epsilon_0$.

Now, the values of the couplings C_k can be deduced from the consistency requirement that they do not disturb the gaplessness of the \hat{a}_k -modes. The corresponding coupling matrix is (for $n_0 = N_c$)

$$\begin{pmatrix} 0 & C_k \\ C_k & \epsilon_0 \sqrt{S} \end{pmatrix}. \quad (30)$$

From the condition that the vanishing gap is offset by at most ϵ_0/\sqrt{S} , it follows that $C_k^2/(\epsilon_0 \sqrt{S}) \lesssim \epsilon_0/\sqrt{S}$, i.e., $C_k \lesssim \epsilon_0$. Thus, due to enormous level splitting, the mixing between the \hat{a}_k and \hat{b}_k is highly suppressed. Correspondingly, the free modes (\hat{b}_k) of the same momenta as the memory modes (\hat{a}_k) stay unoccupied during the time evolution. In other words, the information encoded in the memory modes cannot be transferred to the outgoing radiation since the mixing between the two sets of modes is highly suppressed.

This finding has important implications as it explains *microscopically* [1] why a black hole at the earliest stages of its evolution releases energy but almost no information. This fact is often considered as one of the mysteries of black hole physics. What we are observing is that this is a universal property shared by systems that are in a state

of enhanced memory capacity due to assisted gaplessness. The “secret” lies in a large level splitting between the memory modes subjected to the assisted gaplessness and their free counterparts.

Since due to the above reason the \hat{b}_k -modes will largely stay unoccupied, we do not include them in the numerical simulations. Finally, Since the gravitational interaction scales with energy, we get a bound on the coupling C_0 :

$$C_0 \lesssim \frac{\epsilon_0}{\sqrt{S}}. \quad (31)$$

3 Numerical Time Evolution

For the numerical study, we need to specialize to a particular realization of the system (16). In doing so, we keep in mind the special case of black holes, although our choice of parameters stays much more general. First, we choose the free gaps of all memory modes in both sectors to be equal, $\epsilon_k = \epsilon_{k'} =: \epsilon_m$. Moreover, we assume that all couplings $C_{k,k'}$ and $\tilde{C}_{k,l}$ are of the same order. Therefore, we can represent them as $C_m f_i(k, k')$, where $f_i(k, l)$ take values of order one. It is important that the $f_i(k, l)$ are non-trivial to break the exchange symmetry $\hat{a}_k \leftrightarrow \hat{a}_l$. We choose them so that they essentially take random values in $|f_i(k, l)| \in [0.5; 1]$, with both plus- and minus-sign.² Finally, we note that $\epsilon_0 (\hat{n}_0 + \hat{m}_0)$ corresponds to a conserved quantity. Since as initial states we only consider eigenstates of this operator, it only leads to a trivial global phase and we can leave it out. In turn, we will use ϵ_0 as basic energy unit. We arrive at the Hamiltonian

$$\begin{aligned} \frac{\hat{H}}{\epsilon_0} = & \frac{\epsilon_m}{\epsilon_0} \left(1 - \frac{\hat{n}_0}{N_c} \right) \sum_{k=1}^K \hat{n}_k + \frac{C_0}{\epsilon_0} \left(\hat{a}_0^\dagger \hat{b}_0 + \hat{b}_0^\dagger \hat{a}_0 \right) \\ & + \frac{\epsilon_m}{\epsilon_0} \left(1 - \frac{\hat{n}_0}{N_c - \Delta N} \right) \sum_{k'=1}^{K'} \hat{n}'_{k'} + \frac{C_m}{\epsilon_0} \left\{ \sum_{k=1}^K \sum_{k'=1}^{K'} f_1(k, k') \left(\hat{a}_k^\dagger \hat{a}'_{k'} + \text{h.c.} \right) \right. \\ & \left. + \sum_{k=1}^K \sum_{\substack{l=1 \\ l \neq k}}^K f_2(k, l) \left(\hat{a}_k^\dagger \hat{a}_l + \text{h.c.} \right) + \sum_{k'=1}^{K'} \sum_{\substack{l'=1 \\ l' \neq k'}}^{K'} f_3(k', l') \left(\hat{a}'_{k'}^\dagger \hat{a}'_{l'} + \text{h.c.} \right) \right\}, \quad (32) \end{aligned}$$

where we set $\epsilon_0 = 1$ from here on.

As a final simplification for the numerical study, we truncate all memory modes to qubits. Correspondingly, we consider the initial state

$$|\text{in}\rangle = |N_c, 0, \underbrace{1, \dots, 1}_{N_m}, 0, \dots, 0\rangle, \quad (33)$$

i.e., \hat{n}_0 is populated with N_c particles, \hat{m}_0 is empty and there is one particle in each of the first N_m memory modes.

²Concretely, we choose $f_i(k, l) = \begin{cases} F_i(k, l) - 1 & \text{for } F_i < 0.5 \\ F_i(k, l) & \text{for } F_i \geq 0.5 \end{cases}$, where $F_i(k, l) = (\sqrt{2}(k + \Delta k_i)^3 + \sqrt{7}(l + \Delta l_i)^5) \bmod 1$. Moreover, we set $\Delta k_1 = \Delta k_2 = 1$, $\Delta k_3 = K + 1$, $\Delta l_1 = \Delta l_3 = K + 1$ as well as $\Delta l_2 = 1$.

Unless otherwise stated, the values for the parameters we use are

$$\epsilon_m = \sqrt{20}, \quad N_c = 20, \quad \Delta N = 12, \quad K = K' = 4, \quad C_0 = 0.01, \quad N_m = 2. \quad (34)$$

These parameters define both the Hamiltonian and the initial state, up to a choice of the coupling C_m . We note that we chose $N_m = K/2$ since this corresponds to the most probable state in the limit of large K .³

For the numerical time evolution, we use the approach and software developed in [22]. It is based on a Krylov subspace method and has the strength that it provides a rigorous upper bound on the numerical error, i.e., the norm of the difference between the exact time-evolved state and its numerical approximation. Throughout we set it to be 10^{-6} , with the exception of systems with $K = 8$, for which we use 10^{-5} .

3.1 Possibility of Rewriting

The time evolution of the initial state (33) for different values of C_m is displayed in Fig. 2, where we show the expectation value n_0 of the occupation number of the \hat{n}_0 -mode as well as the expectation value of the total occupation of the first critical sector $\sum_{k=1}^K \hat{n}_k$. For $C_m = 0$ (see Fig. 2a), we can replace $\sum_{k=1}^K \hat{n}_k \rightarrow N_m$ and $\sum_{k'=1}^{K'} \hat{n}'_{k'} \rightarrow 0$ and the system has the analytic solution (9). We observe that the critical sector does not move and the amplitude of oscillations of \hat{n}_0 is strongly suppressed. This is the effect of memory burden [1] discussed before in section 2.2.

For many nonzero values of C_m , the system behaves similarly (see Fig. 2b). Although the time evolution of the system becomes more involved, the amplitude of oscillations of n_0 is still small and the critical sectors remains effectively frozen.

However, there are certain values of C_m for which the system behaves qualitatively differently and the amplitude of oscillations of n_0 increases distinctly, albeit on a significantly longer timescale (see Figs. 2c, 2d). As expected, this behavior is accompanied by a change of the occupation numbers in the critical sector. This can either happen via an instantaneous jump (as in Fig. 2c) or via oscillations that are synchronous with n_0 (as in Fig. 2d). Although the second scenario is more intuitive than the first one, both are in line with our statement that n_0 can only change significantly if also rewriting in the critical sector takes place. Moreover, we note that the occupation transfer and thus the rewriting of information is not complete. We expect that complete rewriting into the second sector of memory modes can be achieved only after including further sectors, to which the $\hat{a}'_{k'}$ -modes can transfer occupation number.

We shall call the values of C_m for which partial rewriting takes place *rewriting values*. For the present values of the remaining parameters (34), such values are rare. In order to illustrate this point, we plot the maximal amplitude of oscillations as a function of C_m in Fig. 3. We remark, however, that for other parameter choices, we have observed much more abundant rewriting values.

³Since K will be mapped onto the entropy of a BH, this reasoning only applies to macroscopic BHs with $M \gg M_p$.

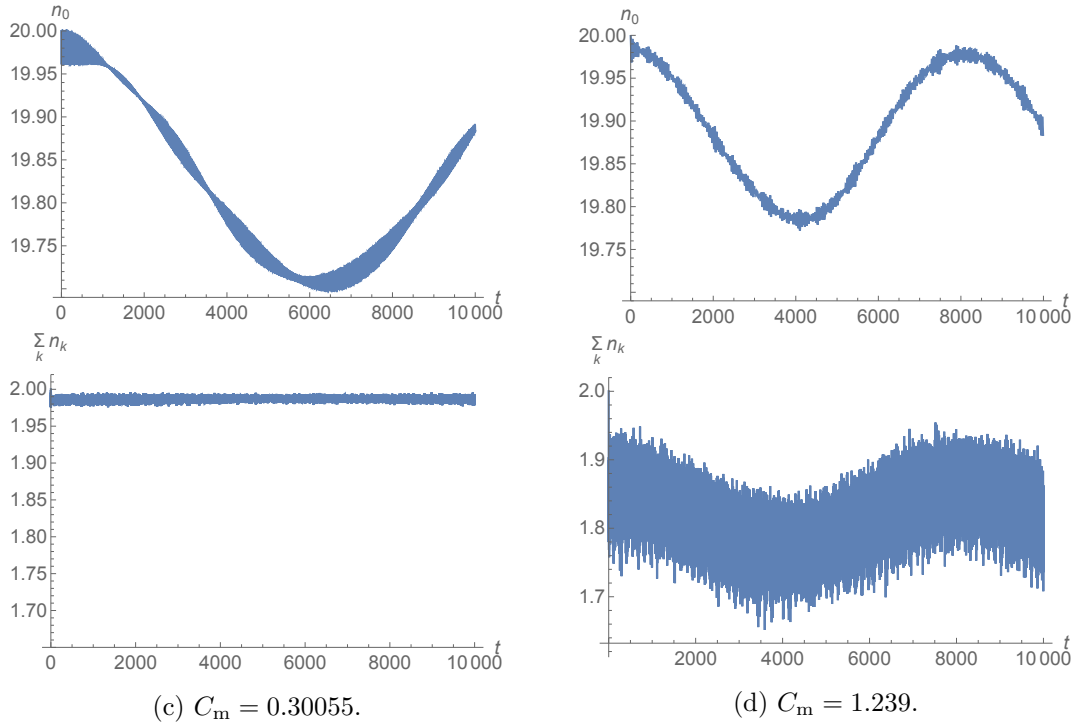
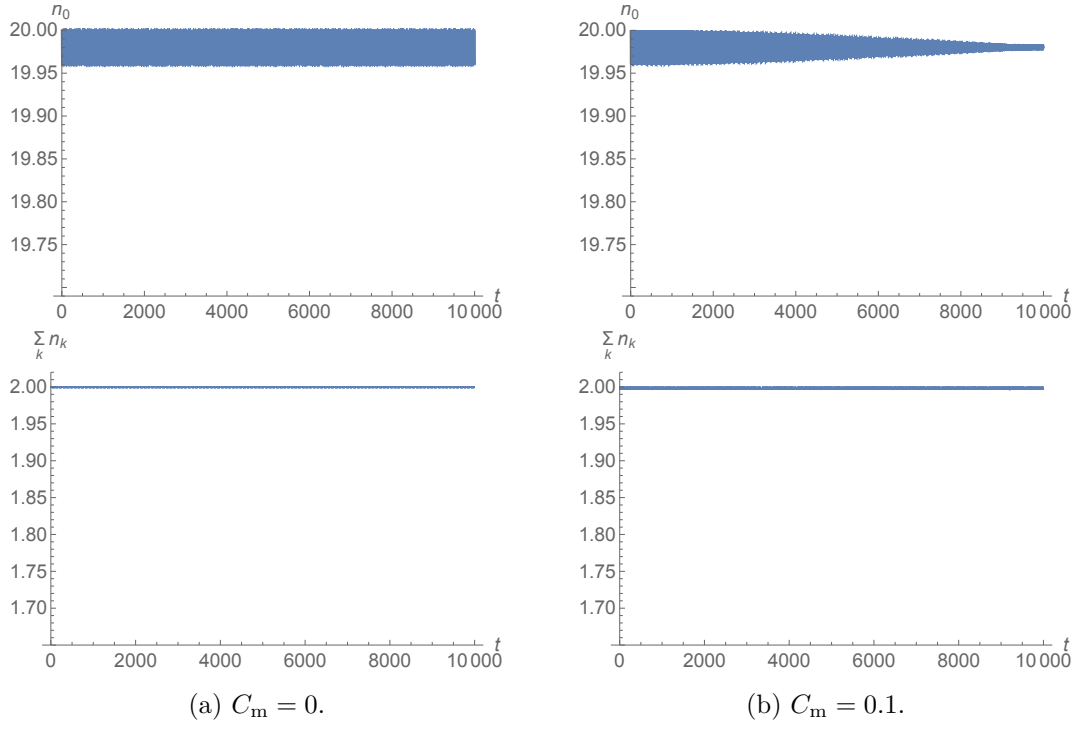


Figure 2: Time evolution of the initial state (33) for different values of C_m . Oscillations on a timescale of order 1 cannot be resolved graphically any more since we show very long timescales. n_0 is the expectation value of the occupation of the mode \hat{a}_0 and $\sum_k n_k$ that of the total occupation in the first critical sector. Time is plotted in units of $\epsilon_0^{-1}\hbar$.

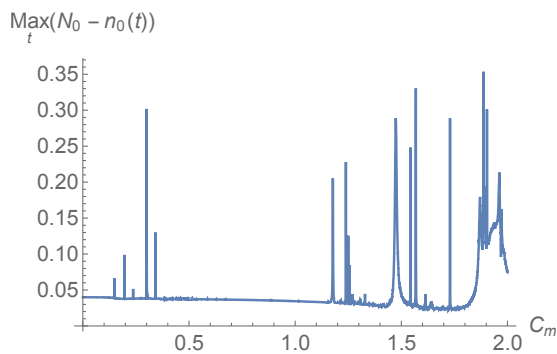


Figure 3: Maximal amplitude of the expectation value of \hat{n}_0 for different values of C_m (with initial state (33)).

3.2 Dependence on System Size

After having seen that rewriting does indeed take place, we now wish to answer the question how this changes as the size of the system increases. In order to answer it, we investigate how the rewriting values of C_m change as we vary the parameters of the Hamiltonian (32). Moreover, it is possible to determine a rate Γ of rewriting as the ratio of the maximal amplitude of n_0 and the timescale on which this maximal value is attained. If we map our system on a decay process, as we have e.g., done in section 2.5, we can identify this rate with the decay rate. We shall also study how the rate Γ changes as we vary the parameters.

As presented in appendix A, the observed scalings for C_m and Γ are as follows:

- The initial occupation number N_c of \hat{n}_0 (which is also the critical occupation at which the first memory sector is gapless):

$$C_m \sim N_c^{-1}, \quad \Gamma \sim N_c^{-1} \quad (35)$$

- The free gap ϵ_m of the memory modes:

$$C_m \sim \epsilon_m^1, \quad \Gamma \sim \epsilon_m^0 \text{ (independent)} \quad (36)$$

- The coupling C_0 of \hat{a}_0 and \hat{b}_0 :

$$C_m \sim C_0^0 \text{ (independent)}, \quad \Gamma \sim C_0^{1.4} \quad (37)$$

- The difference ΔN_c between the critical occupations of \hat{a}_0 making either of the two memory sectors gapless:

$$C_m \sim (\Delta N_c / N_c)^{0.2}, \quad \Gamma \sim (1 - \Delta N_c / N_c) \quad (38)$$

With regard to the K and K' , we can unfortunately only study three values due to numerical limitations, namely $K = K' = 4, 6, 8$. The results are displayed in Fig.

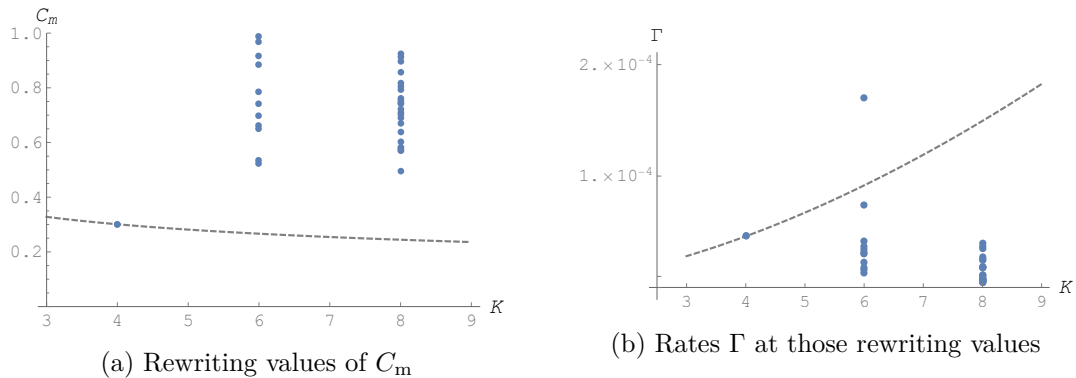


Figure 4: Available data (blue dots) for the rewriting values of C_m and the rates Γ as function of $K = K'$, where we take $N_m = K/2$. The dashed curves are the constraints (44) and (45), that apply to a black hole. We see clear indications that for large black holes, rewriting is not fast enough to reproduce the semiclassical rate of evaporation.

4, where we take $N_m = K/2$. Since we cannot make a precise statement about the dependence on K , we will parameterize it as

$$C_m \sim K^{\beta_C}, \quad \Gamma \sim K^{\beta_\Gamma}. \quad (39)$$

Still, we can try to constrain rewriting, i.e., give a lower bound on C_m and an upper bound on Γ . To this end, we calculate the mean value of C_m for the 11 data points at $K = 6$. In order to obtain a maximally conservative bound, we moreover choose among the results for $K = 8$ the 11 data points with the lowest values of C_m and compute their mean. Performing a fit with the two resulting mean values, we get

$$\beta_C \gtrsim -0.7. \quad (40)$$

We have not included the value at $K = 4$ since doing so would increase β_C . For Γ , we compute the mean value for the 11 data points at $K = 6$. At $K = 8$, we choose the 11 data points with the highest rates and calculate their mean. Fitting the resulting two means together with the rate of the single rewriting value at $K = 4$, we arrive at

$$\beta_\Gamma \lesssim -0.7. \quad (41)$$

In this case, we have not excluded the value at $K = 4$ because this would decrease β_Γ . Even though we have tried to be conservative in our estimates, we must stress that we have far too little data to make any reliable statement. Thus, the true values of β_C and β_Γ might not respect the bounds (40) and (41).

3.3 Application to Black Hole

Now we adapt the parameter choice (27) that corresponds to the case of a black hole. In this situation, only the couplings C_0 and C_m as well as ΔN_c remain independent of S . However, C_0 is related to S through the bound (31), which is specific to black holes. Likewise, the S -dependence of ΔN_c is bounded by the requirement that the separation

of levels should not go to zero for large N_c , i.e., ΔN_c should not decrease with increasing N_c . Using the observed scalings stated in Eqs. (35)-(37), we get for C_m

$$C_m \sim S^{-0.5+\beta_C} (\Delta N_c/S)^{0.2} \gtrsim S^{-0.7+\beta_C}, \quad (42)$$

as well as⁴

$$\Gamma \sim S^{-1.7+\beta_\Gamma}. \quad (43)$$

Eq. (42) shows that in order to satisfy the bound (28) on the S -dependence of C_m , the scaling of C_m with K would be constrained as

$$\beta_C \lesssim -0.3. \quad (44)$$

Analogously, it follows from Eq. (43) that the requirement of reproducing the semiclassical value of the rate, $\Gamma \sim 1$, leads to

$$\beta_\Gamma \gtrsim 1.7. \quad (45)$$

Now we would like to investigate the compatibility of the numerical results for K -variation with the bounds in Eqs. (44) and (45). Firstly, we compare the actual results for $K = 6, 8$ with the expectation for $K = 6, 8$ based on the result for $K = 4$ and a scaling saturating the bounds Eqs. (44) and (45). The resulting functions are plotted in Fig. 4. We observe that although many more rewriting values exist at higher K , none of them satisfies both the constraints (44) and (45).⁵

As a different method of analysis, we can compare the bounds (44) and (45) with the estimates (40) and (41). We observe that β_C might be small enough, but β_Γ is vastly different. These are clear indications that for large black holes rewriting of information from one memory sector to another one cannot be efficient enough to reproduce the semiclassical rate of particle creation, $\Gamma \sim 1$. As far as we can numerically access the system, we therefore conclude that even if rewriting takes place, the semiclassical description breaks down as soon as memory burden sets in.

We expect the semiclassical approximation to be valid as long as a newly created black hole has not lost a sizable fraction of its mass. In the absence of sufficiently fast rewriting, the model (32), which we have studied here, does not fulfill this requirement because it would lead to an immediate deviation from the semiclassical rate of particle production. Therefore, an effective description of black hole evolution must realize an appropriate delay of the onset of the memory burden effect. As reviewed in 2.2, the model (12) (with a parameter choice $p \gg 1$) achieves such a delay. It can do so at most until the master mode has lost on the order of half of its initial occupation, and, correspondingly, until the black hole has lost on the order of half of its mass.

We can give a quantitative estimate of how strong the slowdown is at that point, assuming that the rewriting rate after the onset of backreaction in the system (12) (with a parameter value $p \gg 1$ and including the coupling to another set of memory

⁴Since $\Delta N_c/S \rightarrow 0$, the rate Γ becomes independent of ΔN_c .

⁵In fact, none of them fulfills either condition, except for one data point at $K = 6$. It has a sufficiently high rate, but its coupling strength $C_m = 0.74$ is far too big to satisfy the bound (44).

modes) behaves analogously to the system investigated here. To this end, we first note that $C_0 \sim 1/S$ is required in order to reproduce the semiclassical rate of Hawking evaporation, $\Gamma \sim 1$, during the initial evolution before the onset of memory burden. Consequently, Eq. (43) gets modified:

$$\Gamma \sim S^{-2.4+\beta_\Gamma}. \quad (46)$$

As explained, we cannot determine β_Γ due to numerical limitations. Still, we can try to give a bound on it. Since we clearly see no indications that the rates increase with K (see Eq. (41)), we can conservatively estimate that $\beta_\Gamma < 0$. Then we obtain

$$\Gamma \lesssim \frac{1}{S^2}. \quad (47)$$

Thus, evaporation has to slow down drastically at the latest after the black hole lost on the order of half of its initial mass.

3.4 Regime After Metamorphosis

In the following, we will discuss scenarios of BH evolution beyond half-decay that are consistent with the above finding. In the standard semiclassical treatment, the evaporation process of a black hole is taken to be *self-similar*, i.e., it is assumed to be well described simply by a time-dependent mass $M(t)$ which in each moment of time determines the Schwarzschild radius and the temperature as $r_g = 2G_N M(t)$ and $T = (8\pi G_N M(t))^{-1}$, respectively. This leads to the picture of a thermal emission spectrum shifting with the growing temperature as the evaporation proceeds. Thus, the assumption is that a *classical* black hole with each *quantum* emission evolves into a *classical* black hole of a lower mass. This picture is widely accepted, despite the fact that there exist no self-consistent semi-classical calculation giving such a time evolution.

It is quite contrary [23]: This picture has a built-in measure of its validity since the above equation, together with $\dot{M} \sim r_g^{-2}$, leads to $\dot{T}/T^2 \sim 1/S$. This quantity sets the lower bound on the deviation from thermality. It vanishes only in strict semi-classical limit $G_N \rightarrow 0$, $M \rightarrow \infty$, $r_g = \text{finite}$. It is important to note that in this limit $S \rightarrow \infty$. Therefore, the standard Hawking result is exact. However, for finite mass black holes and non-zero G_N , the deviations from thermal spectrum are set by $1/S$.

Already this fact tells us that it is unjustified to use the self-similar approximation over timescales comparable with black hole half-decay, $\tau \sim S r_g$. Indeed, without knowing the microscopic quantum theory, one can never be sure that the semi-classical approximation is not invalidated due to a build-up of quantum back-reaction over the span of many emissions.

As microscopic theory tells us [3, 12, 13, 15], this is exactly what is happening: At the latest by the time a black hole loses of order of half of its mass, the back-reaction is so strong that the semiclassical treatment can no longer be used.⁶ In particular, the

⁶Self-similarity is only recovered in the semiclassical limit $N_c \rightarrow \infty$ [24].

remaining black hole state is fully entangled after losing on the order of half of its constituents.

The present study reveals a new microscopic meaning of the quantum back reaction. Namely, being states of maximal memory capacity, the black holes are expected to share the universal property of memory burden. Due to this phenomenon, the black hole evaporation rate must change drastically after losing half of its mass. What happens beyond this point can only be a subject to a guess work. However, given the tendency that the memory burden resist the quantum evaporation, the two possible outcomes are: 1) A partial stabilization by slowing down the evaporation; 2) Classical disintegration into some highly non-linear gravitational waves. The second option becomes possible because after the breakdown of the description in terms of a classical black hole, we cannot exclude any more that the system exhibits a classical instability. Obviously, there could be a combination of the two options, where a prolonged period of slow evaporation transits into a classical instability. In the following, we shall focus on the first option as being the most interesting for the dark matter studies.

Thus, motivated from our analysis of the prototype model, we shall adopt that the increased lifetime due to the slowdown is

$$\tilde{\tau} \gtrsim r_g S^{1+k}, \quad (48)$$

where k indicates the power of additional entropy suppression of the decay rate as compared to the semiclassical rate, $\Gamma \sim r_g^{-1}$. Although the spectrum is no longer thermal, we shall assume that the mean wavelength of quanta emitted during this stage is still on the order of the initial Schwarzschild radius $\sim r_g$, as long as the mass is still on the order of the initial mass. We must stress, however, that we cannot exclude that the black hole starts emitting much harder quanta after memory burden has set in. In particular, as the gap increases, the memory modes become easier-convertible into their free counterparts. This conversion is likely a part of the mechanism by which the information starts getting released after the black hole's half decay.

4 Small Primordial Black Holes as Dark Matter

The possible stabilization of black holes by the burden of memory could have interesting consequences for the proposal that primordial black holes (PBHs) constitute dark matter [25–28]. Of course, the full investigation of this parameter space requires more precise information about the behavior of black holes past their naive half life. Below, we first give a short qualitative discussion of how some of the bounds on primordial black holes change in this case. Subsequently, we provide a few quantitative considerations for one exemplary black hole mass.

4.1 Effects on Bounds

There exist many different kinds of constraints on the possible abundance of PBHs (see [29, 30] for a review). However, the strength and/or the range of many of those

constraints are based on the semiclassical approximation for BH evaporation, i.e., Hawking evaporation is assumed throughout the decay. Therefore, a slowdown due to the backreaction in form of memory burden, which sets in after the half-decay, affects the landscape of constraints quite dramatically.

If the validity of the semiclassical approximation is assumed throughout the whole decay process, all PBH with masses $M \lesssim M_* \equiv 5 \cdot 10^{14} g$ would have completely evaporated by the present epoch [30]. In contrast, such small PBHs can survive until today if evaporation slows down after half-decay. Thus, many of the constraints on the initial abundance of PBHs with masses $M \lesssim M_*$ are altered. In particular, a new window for PBHs as DM is opened up for some values of the mass below M_* .

For example, we can consider constraints from the galactic gamma-ray background, following [31]. Since the spectrum of photons observed due to PBHs clustering in the halo of our galaxy is dominated by their instantaneous emission, the range of the related constraints in the semiclassical picture applies to black holes with mass $M \gtrsim M_*$, with the strongest constraints coming from M close to M_* (since they would be in their final, high-energetic stage of evaporation today). On the one hand, a slowdown significantly alleviates the constraint around M_* since such black holes would now be in their second, slow phase of evaporation. On the other hand, because black holes with masses below M_* could survive until today, the galactic gamma-ray background would lead to new constraints on their abundance. At the same time, the fact that these black holes emit energetic quanta opens up a possibility to search for them via very high-energetic cosmic rays. Below we discuss this point in more detail.

As a different example, we consider constraints from BBN, as were studied in [32]. In the semiclassical picture, PBHs of mass smaller than about $M_N \equiv 10^{10} g$ would have evaporated until then. Therefore, such black holes are typically considered to be unconstrained by BBN. In contrast, a slowdown would cause some PBHs with $M \lesssim M_N$ to still exist at that epoch. Therefore, BBN in principle leads to new constraints on such PBHs. However, the constraints are expected to be mild, since PBHs would already be in their second, slow phase of evaporation. On the other hand, the strong constraints on $M \sim M_N$ associated with the final stage of evaporation in the Hawking-picture is alleviated. Finally, the bound due to BBN on PBHs of masses $M \gg M_N$ is the same in the semiclassical and our picture because those black holes are in the early stages of evaporation during BBN.

4.2 Specific Example

In the following, we consider an exemplary scenario, in which small PBHs of mass below M_* appear to be able to constitute all of dark matter. It should be clear that we make no attempt to cover the whole spectrum of constraints or the whole range of masses, and content ourselves with rough estimates. We consider a monochromatic PBH mass spectrum with $M \sim 10^8 g$. Moreover, we need to specify how strong the slowdown is after half decay. Based on our numerical finding (47), we assume that the rate $\tilde{\Gamma}$ is suppressed by two powers of the entropy: $\tilde{\Gamma} \sim r_g^{-1}/S^2$. Correspondingly, we have $k = 2$ in Eq. (48), i.e., the lifetime $\tilde{\tau}$ is prolonged as $\tilde{\tau} \gtrsim S^2 \tau$, where τ is the standard estimate

based on extrapolation of Hawking's result. This leads to $\tilde{\tau} \gtrsim 10^{49}$ s (see [30] for τ), which is longer than the age of the Universe by many orders of magnitude.

There are two kinds of constraints on the PBHs that we consider. Bounds of the first type are independent of the fact that the PBHs evaporate, i.e., they are identical to the ones for MACHOs of the same mass. We are not aware of relevant constraints for masses as low as $M \sim 10^8 g$ (see e.g., [30, 33]).⁷ The second kind of bounds is due to the fact that, although with a suppressed rate, the PBHs still evaporate.

As explained above, the energy of emitted particles is expected to be around the initial black hole temperature, $T_{\text{BH}} = M_p^2/(8\pi M) \sim 10^5$ GeV. Assuming that the galactic halo is dominated by the PBHs, the diffuse galactic photon flux due to the PBHs can be roughly estimated as

$$\Phi \sim n_{\text{BH}} R \tilde{\Gamma} \sim 10^{-34}/(\text{cm}^2\text{s}), \quad (49)$$

where $R \sim 2 \cdot 10^{24}$ cm is the typical radius of the Milky Way halo and n_{BH} is the galactic number density of PBHs. We can estimate the latter in terms of the mass of our galaxy $M_{\text{MW}} \sim 2 \cdot 10^{42}$ kg as $n_{\text{BH}} \sim M_{\text{MW}}/(MR^3)$. This corresponds to one particle hitting the surface of the earth approximately every 10^8 years. Clearly, it is impossible to observationally exclude such a low flux.⁸ Moreover, one can wonder if the secondary flux, which predominantly comes from the decay of pions, can change the above conclusion. The answer is negative since the corresponding rate $\tilde{\Gamma}_S$ is only slightly higher than the one for primary emission, $\tilde{\Gamma}_S \sim 10\tilde{\Gamma}$ (see [31]).

Moreover, we can turn to constraints from the extragalactic gamma-ray background. Assuming that cold DM is dominated by PBHs of mass M , one can roughly estimate for the flux due to secondary photons⁹ (see [32]):

$$\Phi \sim \frac{\rho_{\text{DM}}}{M} \tilde{\Gamma} t_0 \sim 10^{-31}/(\text{cm}^2\text{s}), \quad (50)$$

where $\rho_{\text{DM}} \sim 2 \cdot 10^{-30}$ g/cm³ is the present energy density of dark matter in the Universe and $t_0 \sim 4 \cdot 10^{17}$ s is the age of the Universe. Again, this flux is unobservably small.

Finally, the contribution from the considered PBHs to cosmic rays other than photons can be expected not to exceed significantly the photonic flux, in which case no bound would result from direct detection of other particles, either.

In conclusion, from the exemplary constraints considered above, the numerical example of PBHs of mass $M \sim 10^8 g$ passes an immediate test to be able to account for all DM. As stated above, a more complete analysis remains to be done.

We finish the section by making a general remark. The stabilized black holes can be detected via their emission but also via a direct encounter with earth, through gravitational or seismic disturbance. The latter possibility for standard PBH has been discussed in [37]. In the present context, the encounter becomes much more frequent and

⁷Constraints would be similar to the ones on N-MACHOs [34].

⁸We are not aware of an observational lower bound on the diffuse galactic gamma-ray flux at photon energies $E_\gamma \sim 10^5$ GeV. For $E_\gamma \sim 10^3$ GeV, the observed flux is of order $10^{-10}/(\text{cm}^2\text{s})$ [35].

⁹The primary photons would effectively be screened by a cosmic gamma-ray horizon (see e.g., [36])

for certain masses the detection through a direct encounter could in principle become more probable than by emission spectrum.¹⁰

5 Summary and Conclusions

5.1 Stabilization by Memory Burden

A state around which gapless modes exist possesses an enhanced capacity of memory storage since information patterns can be recorded in the excitations of the gapless degrees of freedom at a very low energy cost. However, the stored information backreacts on the evolution of the system and ties it to its initial state. This is the effect of memory burden [1].

In this paper, we have investigated if memory burden can be avoided once another set of degrees of freedom exists, which becomes gapless for a different state of the system and to which the stored information can be transferred. We refer to this process as rewriting. In a prototype model, we have found a positive answer. For certain values of the parameters, a non-trivial evolution in the form of rewriting is indeed possible. It turns out that the timescale of this process is very long and we have studied how it depends on the various parameters of the system.

We can choose the parameters of our prototype model in such a way that it reproduces the information-theoretic properties of a black hole, in particular its entropy. In this case, we have concluded that as far as we can numerically access the system, rewriting happens significantly too slowly to match the semiclassical rate of particle production. This strongly indicates that evaporation has to slow down drastically at the latest after the black hole has lost on the order of half its initial mass.

This could open up a new parameter space for primordial black holes as dark matter candidates. For sufficiently low masses, those black holes would evaporate on a timescale shorter than the age of the Universe if Hawking's semiclassical calculation were valid throughout their lifetime. It is often assumed that this is the case so that the corresponding mass ranges are considered as excluded.

By contrast, a significant slowdown of the rate of energy loss, as is e.g., displayed in Eq. (47), allows the lifetimes of such PBHs to be much longer so that they can still exist today. In this case, small PBHs become viable dark matter candidates. We have qualitatively discussed how some of the constraints change and studied a concrete example. A full investigation of parameter space remains to be done.

Our findings also have interesting implications for de Sitter space. In [2], we have already discussed the role of memory burden for this system and how it leads to primordial quantum memories that are sensitive to the whole inflationary history and not only the last 60 e-foldings. Since the information-theoretic properties of de Sitter are fully analogous to those of black holes, our results imply that avoiding memory burden

¹⁰We thank Florian Kühnel for comments on this issue.

by rewriting the stored information cannot be efficient for de Sitter, either. This further supports the conclusions of [2].

5.2 Black Hole Metamorphosis After Half Decay

Finally, our analysis adds paint to the quantum picture of black holes. It has been standard to assume that black hole evaporation is *self-similar* all the way until the black hole reaches the size of the cutoff scale. For example, after a solar mass black hole loses, say, 90 percent of its initial mass, the resulting black hole is commonly believed to be indistinguishable from a young black hole with 0.1 solar mass. In other words, the standard assumption is that a black hole at any stage of its existence has no memory about its prior history. This assumption is based on naive extrapolation of Hawking's *exact* semi-classical computation towards arbitrary late stages of black hole evaporation. However, this extrapolation unjustly neglects the quantum back-reaction that alters the state of a black hole. The lower bound on the strength of the back-reaction effect can be derived using solely the self-consistency of Hawking formula and is $\sim 1/S$ per each emission [23]. This fact already gives a strong warning sign that we cannot extrapolate the semi-classical result over timescales of order S emissions.

However, only in a microscopic theory such as the quantum N -portrait [3] it is in principle possible to account for back-reaction properly and to understand its physical meaning. This theory predicts [12–16] that semiclassical treatment cannot be extrapolated beyond the point when the black hole loses half of its mass. The physical meaning of this effect is very transparent. Indeed, at this point the black hole loses half of its graviton constituents that leave the bound state in form of the Hawking quanta. The quantum state of the remaining $\sim N_c/2$ gravitons is fully entangled and is no longer representable as approximately-classical coherent state.

In the present paper, we have identified another very explicit source of backreaction in form of the memory burden effect described earlier in [1,2]. This effect shows that black hole evaporation cannot be self-similar and that old black holes are drastically different from the younger siblings of equal mass. That is, the memory burden results in a quantum hair that exerts a strong influence at later stages. This provides a concrete mechanism for the release of information after Page's time [38]. Note, such a quantum hair is not constrained by the classical no-hair theorems [39].

While it is evident that the memory burden resists to quantum decay of a black hole, the further evolution requires a more detailed study. In particular, it is not excluded that some sort of a classical instability can set in after half-decay. Our prototype models are not powerful enough for either capturing such instabilities or excluding them. However, they clearly indicate the tendency of dramatic slow-down of the quantum decay. Our speculations about the small black holes as dark matter candidates are based on this evidence. Nevertheless, the possibility of developing a classical instability after the suppression of the quantum emission remains feasible and must be investigated seriously. An interesting avenue in this direction would be an experimental simulation of the effect in laboratory, since the states of enhanced memory capacity can be achieved in simple setups with cold bosons (see [10] and references therein).

Another promising approach could be to use the recently established connection between the saturation of the information storage capacity and unitarity of scattering amplitudes in generic quantum field theories [11]. All studied saturated objects exhibit close similarities with black holes and are also subjected to the effect of memory burden. So the question about the classical instability versus stabilization can be addressed by studying the latest stages of their time-evolution.

In conclusion, the memory burden backreaction opposes the quantum decay and the resistance becomes maximal by the time the black hole loses half of its mass. This behavior and whatever happens after is very different from the standard semi-classical picture and changes our understanding of black holes.

Acknowledgements

It is a pleasure to thank Florian Kühnel for comments. This work was supported in part by the Humboldt Foundation under Humboldt Professorship Award, by the Deutsche Forschungsgemeinschaft (DFG, German Research Foundation) under Germany's Excellence Strategy - EXC-2111 - 390814868, Munich Center for Quantum Science and Technology, Germany's Excellence Strategy under Excellence Cluster Origins as well as ERC-AdG-2015 grant 694896.

A Finding Parameter Scalings

In order to determine how the rewriting values of C_m and the corresponding rates Γ scale with the parameter $X \in \{N_c, \epsilon_m, C_0, \Delta N_c, K\}$, the system has been time evolved with different X , with the remaining parameters fixed at the values given in (34). For each X -value, the time evolutions have been done for many couplings $C_m \in [0, 1]$ (or a larger interval), where we used a sampling step of $\delta C_m = 10^{-3}$ or smaller.

We have defined a rewriting value of C_m as a value of C_m for which the amplitude of n_0 exceeds the amplitude of n_0 in the free case, i.e., the case of $C_m = 0$, by a factor of at least 1.2. For neighboring rewriting values (i.e., separated only by the increment δC_m), we only considered the one with the highest value of Γ . Around this value, we again performed time evolutions with a smaller sampling step of $\delta C_m = 5 \cdot 10^{-5}$. The reason why we did so is that the rate depends on C_m very sensitively. Finally, we always selected the point with the highest rate.

In the following, we show the plots containing the data as well as fits for the individual scalings and further elaborate on our procedure.

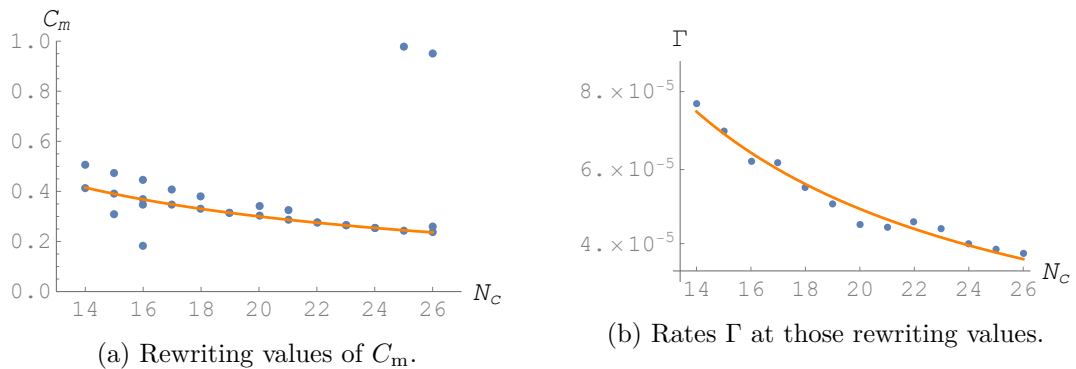


Figure 5: Data and fits for the rewriting values of C_m and the rates Γ as function of N_c . ΔN_c has been varied to keep $N_c/\Delta N_c$ fixed.

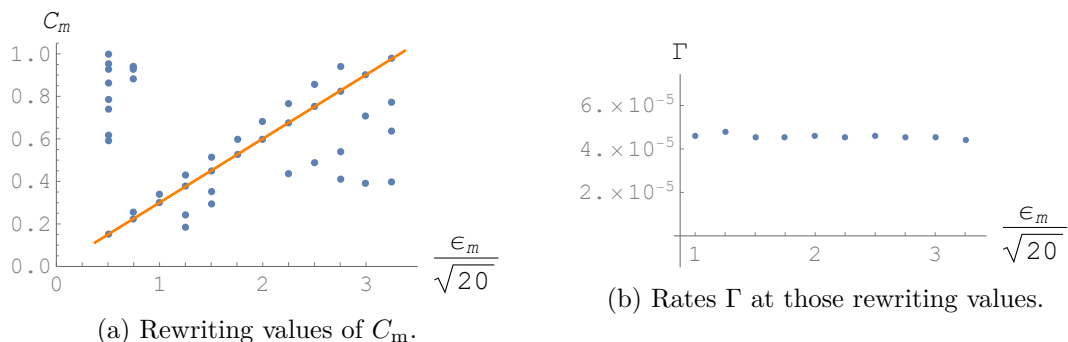


Figure 6: Data and fit for the rewriting values of C_m and the rates Γ as function of ϵ_m .

A.1 N_c -Scaling

The data used to determine the scaling of (C_m, Γ) with N_c is shown in Fig. 5. The N_c -variation has been done varying also ΔN_c , s.t. $N_c/\Delta N_c$ stays fixed. The function fitted to the rewriting values is $f_C(N_c) = a \left(\frac{N_c}{22}\right)^{-b}$, with the fit result $a \approx 0.275$ and $b = 0.911$. The function fitted to the rates is $f_\Gamma(N_c) = A \left(\frac{N_c}{22}\right)^{-B}$, with the fit result $A \approx 4.46 \cdot 10^{-5}$ and $B = 1.14$.

A.2 ϵ_m -Scaling

The data used to determine the scaling of (C_m, Γ) with ϵ_m is shown in Fig. 6. The function fitted to the rewriting values is $f_C(\epsilon_m) = a\epsilon_m$, with the fit result $a \approx 0.300$. We observe that the scaling of the rate Γ with ϵ_m is negligible compared to its scaling with other parameters.

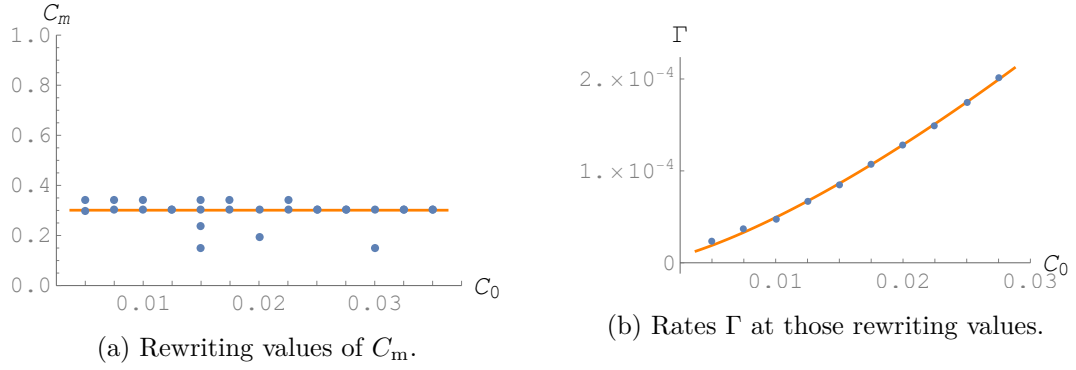


Figure 7: Data and fits for the rewriting values of C_m and the rates Γ as function of C_0 .

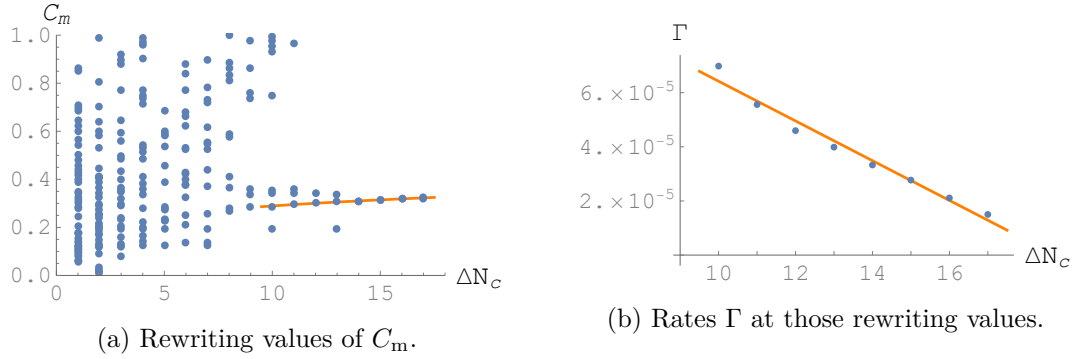


Figure 8: Data and fits for the rewriting values of C_m and the rates Γ as function of ΔN_c .

A.3 C_0 -Scaling

The data used to determine the scaling of (C_m, Γ) with C_0 is shown in Fig. 7. For the scaling of the rewriting values with C_0 , we observe that it is negligible compared to the scaling with other parameters. The function fitted to the rates is $f_\Gamma(C_0) = AC_0^B$, with the fit result $A \approx 2.85 \cdot 10^{-2}$ and $B = 1.38$.

A.4 ΔN_c -Scaling

The data used to determine the scaling of (C_m, Γ) with ΔN_c is shown in Fig. 8. The function fitted to the rewriting values is $f_C(\Delta N_c) = a \left(\frac{\Delta N_c}{12} \right)^b$, with the fit result $a \approx 0.300$ and $b = 0.207$.¹¹ The function fitted to the rates is $f_\Gamma(\Delta N_c) = A \left(1 - B \frac{\Delta N_c}{20} \right)$, with the fit result $A \approx 1.38 \cdot 10^{-4}$ and $B = 1.07$.

¹¹A second scaling behavior seems to exist with $b = -0.130$. Since $\Delta N_c/N_c \rightarrow 0$ in the limit of a large system, this scaling would be even less favorable for rewriting and we consequently do not consider it.

A.5 K -Scaling

When investigating how the system depends on K , the problem is that the size of the Hilbert space grows exponentially with the number of modes. Therefore, only values up to $K = 8$ are numerically accessible. In order to be insensitive to effects of changing the relative occupation of the memory modes, we moreover restrict ourselves to $N_m = K/2$. Since the system appears to behave in a non-generic way for $K = 2$, we are only left with three datasets corresponding to $K = 4, 6, 8$.

An additional difficulty arises from the fact that time evolutions for $K = 8$ are already very time-consuming. Since many rewriting values exist at $K = 8$, it is not feasible to perform fine scans, which are required for a precise determination of the rate, around each of them. To overcome this problem, we have selected a particular subset of rewriting values and only used them for the subsequent analysis. Namely, only those rewriting values of C_m have been taken into account which have at least one neighboring rewriting value, i.e., a rewriting value separated solely by the increment $\delta C_m = 10^{-3}$. Of course, we have applied the same selection procedure for $K = 4$ and $K = 6$. Only the selected rewriting values are displayed in Fig. 4, and only for those the rate has been determined by means of a finer scan.

References

- [1] G. Dvali, *A Microscopic Model of Holography: Survival by the Burden of Memory*, [arXiv:1810.02336](#) [hep-th].
- [2] G. Dvali, L. Eisemann, M. Michel, and S. Zell, *Universe's Primordial Quantum Memories*, *J. Cosmol. Astropart. Phys.* **1903** (2019) 010, [arXiv:1812.08749](#) [hep-th].
- [3] G. Dvali and C. Gomez, *Black Hole's Quantum N-Portrait*, *Fortschr. Phys.* **61** (2013) 742, [arXiv:1112.3359](#) [hep-th].
- [4] G. Dvali and C. Gomez, *Black Holes as Critical Point of Quantum Phase Transition*, *Eur. Phys. J. C* **74** (2014) 2752, [arXiv:1207.4059](#) [hep-th].
- [5] G. Dvali, A. Franca, C. Gomez, and N. Wintergerst, *Nambu-Goldstone Effective Theory of Information at Quantum Criticality*, *Phys. Rev. D* **92** (2015) no. 12, 125002, [arXiv:1507.02948](#) [hep-th].
- [6] G. Dvali and M. Panchenko, *Black Hole Type Quantum Computing in Critical Bose-Einstein Systems*, [arXiv:1507.08952](#) [hep-th]; *Black Hole Based Quantum Computing in Labs and in the Sky*, *Fortschr. Phys.* **64** (2016) no. 8-9, 569, [arXiv:1601.01329](#) [hep-th].
- [7] G. Dvali, *Critically excited states with enhanced memory and pattern recognition capacities in quantum brain networks: Lesson from black holes*, [arXiv:1711.09079](#) [quant-ph].

- [8] G. Dvali, *Area Law Micro-State Entropy from Criticality and Spherical Symmetry*, Phys. Rev. D. **97** (2018) no. 10, 105005, [arXiv:1712.02233 \[hep-th\]](#).
- [9] G. Dvali, *Black Holes as Brains: Neural Networks with Area Law Entropy*, Fortschr. Phys. **66** (2018) no. 4, 1800007, [arXiv:1801.03918 \[hep-th\]](#).
- [10] G. Dvali, M. Michel, S. Zell, *Finding Critical States of Enhanced Memory Capacity in Attractive Cold Bosons*, Eur. Phys. J. Quantum Technology **6** (2019) no. 1, [arXiv:1805.10292 \[quant-ph\]](#).
- [11] G. Dvali, *Area Law Saturation of Entropy Bound from Perturbative Unitarity in Renormalizable Theories*, [arXiv:1906.03530 \[hep-th\]](#);
G. Dvali, *Unitarity Entropy Bound: Solitons and Instantons*, [arXiv:1907.07332 \[hep-th\]](#);
G. Dvali, *Entropy Bound and Unitarity of Scattering Amplitudes*, [arXiv:2003.05546 \[hep-th\]](#).
- [12] G. Dvali and C. Gomez, *Black Hole's $1/N$ Hair*, Phys. Lett. B **719** (2013), 419, [arXiv:1203.6575 \[hep-th\]](#).
- [13] G. Dvali and C. Gomez, *Black Hole Macro-Quantumness*, [arXiv:1212.0765 \[hep-th\]](#).
- [14] G. Dvali, D. Flassig, C. Gomez, A. Pritzel and N. Wintergerst, *Scrambling in the Black Hole Portrait*, Phys. Rev. D **88** (2013) no.12, 124041, [arXiv:1307.3458 \[hep-th\]](#).
- [15] G. Dvali and C. Gomez, *Quantum Compositeness of Gravity: Black Holes, AdS and Inflation*, JCAP **01** (2014), 023 [[arXiv:1312.4795 \[hep-th\]](#)].
- [16] G. Dvali, C. Gomez and S. Zell, *Quantum Break-Time of de Sitter*, JCAP **06** (2017), 028, [arXiv:1701.08776 \[hep-th\]](#).
- [17] G.W. Gibbons, S.W. Hawking, *Cosmological Event Horizons, Thermodynamics, and Particle Creation*, Phys. Rev. D. **15** (1977) 2738.
- [18] T. Tao, *Topics in random matrix theory*, American Mathematical Society, Graduate studies in mathematics **132** (2012).
- [19] G. Dvali, *Classicalization Clearly: Quantum Transition into States of Maximal Memory Storage Capacity*, [arXiv:1804.06154 \[hep-th\]](#).
- [20] J. D. Bekenstein, *Black holes and entropy*, Phys. Rev. D **7** (1973) no. 8, 23336.
- [21] S. Hawking, *Particle Creation by Black Holes*, Commun. Math. Phys. **43** (1975), 199.
- [22] L. Eisemann, M. Michel, and S. Zell, *Numerical Time Evolution for Generic Quantum Systems With Rigorous Error Bound*, to appear.
- [23] G. Dvali, *Non-Thermal Corrections to Hawking Radiation Versus the Information Paradox*, Fortsch. Phys. **64** (2016), 106, [arXiv:1509.04645 \[hep-th\]](#).

- [24] G. Dvali, C. Gomez, *Landau-Ginzburg limit of black hole's quantum portrait: Self-similarity and critical exponent*, Phys. Lett. B **716** (2012), 240, [arXiv:1203.3372](#) [[hep-th](#)];
V.F. Foit, N. Wintergerst, *Self-similar Evaporation and Collapse in the Quantum Portrait of Black Holes*, Phys. Rev. D **92** (2015) no. 6, 064043, [arXiv:1504.04384](#) [[hep-th](#)].
- [25] Y.B. Zel'dovich, I.D. Novikov, *The Hypothesis of Cores Retarded during Expansion and the Hot Cosmological Model*, Sov. Astron. **10** (1967), 602.
- [26] S. Hawking, *Gravitationally collapsed objects of very low mass*, Mon. Not. Roy. Astron. Soc. **152** (1971), 75.
- [27] B. J. Carr and S. Hawking, *Black holes in the early Universe*, Mon. Not. Roy. Astron. Soc. **168** (1974), 399.
- [28] G. F. Chapline, *Cosmological effects of primordial black holes*, Nature **253** (1975), 251.
- [29] B. Carr, F. Kühnel and M. Sandstad, *Primordial Black Holes as Dark Matter*, Phys. Rev. D **94** (2016) no. 8, 083504, [arXiv:1607.06077](#) [[astro-ph.CO](#)].
- [30] B. Carr, K. Kohri, Y. Sendouda and J. Yokoyama, *Constraints on Primordial Black Holes*, [arXiv:2002.12778](#) [[astro-ph.CO](#)].
- [31] B. Carr, K. Kohri, Y. Sendouda and J. Yokoyama, *Constraints on primordial black holes from the Galactic gamma-ray background*, Phys. Rev. D **94** (2016) no.4, 044029, [arXiv:1604.05349](#) [[astro-ph.CO](#)].
- [32] B. Carr, K. Kohri, Y. Sendouda and J. Yokoyama, *New cosmological constraints on primordial black holes*, Phys. Rev. D **81** (2010), 104019, [arXiv:0912.5297](#) [[astro-ph.CO](#)].
- [33] C. Alcock *et al.* [MACHO and EROS], *EROS and MACHO combined limits on planetary mass dark matter in the galactic halo*, Astrophys. J. Lett. **499** (1998), L9, [arXiv:astro-ph/9803082](#) [[astro-ph](#)].
- [34] G. Dvali, E. Koutsangelas and F. Kühnel, *Compact Dark Matter Objects via N Dark Sectors*, Phys. Rev. D **101** (2020), 083533, [arXiv:1911.13281](#) [[astro-ph.CO](#)].
- [35] M. Ackermann *et al.* [Fermi-LAT], *The spectrum of isotropic diffuse gamma-ray emission between 100 MeV and 820 GeV*, Astrophys. J. **799** (2015), 86, [arXiv:1410.3696](#) [[astro-ph.HE](#)].
- [36] T. Kneiske, K. Mannheim and D. Hartmann, *The Gamma-ray horizon*, AIP Conf. Proc. **587** (2001) no.1, 358.
- [37] Y. Luo, S. Hanasoge, J. Tromp, and F. Pretorius *Detectable seismic consequences of the interaction of a primordial black hole with Earth*, Astrophys. J. **751** (2012), 16. [arXiv:1203.3806](#) [[astro-ph.CO](#)].

- [38] D.N. Page, *Information in black hole radiation*. Phys. Rev. Lett. **71** (1993), 3743, [arXiv:hep-th/9306083](#).
- [39] R. Ruffini and J.A. Wheeler, *Introducing the black hole*, Phys. Today **24** (1971) no. 1, 30 ;
- J. Hartle, *Long-Range Neutrino Forces Exerted by Kerr Black Holes*, Phys. Rev. D **3** (1971), 2938;
- J.D. Bekenstein, *Transcendence of the Law of Baryon-Number Conservation in Black-Hole Physics*, Phys. Rev. Lett. **28** (1972), 452;
- J.D. Bekenstein, *Nonexistence of Baryon Number for Static Black Holes*, Phys. Rev. D **5** (1972), 1239 ;
- J.D. Bekenstein, *Nonexistence of Baryon Number for Black Holes. II*, Phys. Rev. D **5** (1972), 2403 ;
- C. Teitelboim, *Nonmeasurability of the baryon number of a black-hole*, Lett. Nuovo. Cim. **3** (1972), 326 ;
- C. Teitelboim, *Nonmeasurability of the lepton number of a black hole* Lett. Nuovo. Cim. **3** (1972), 397.